The EMBO Journal Vol. 20 No. 1 & 2 pp. 27–39, 2001

Decreased nuclear β-catenin, tau hyperphosphorylation and neurodegeneration in GSK-3β conditional transgenic mice

José J.Lucas, Félix Hernández, Pilar Gómez-Ramos[1], María A.Morán[1], René Hen[2] and Jesús Avila[3]

Centro de Biología Molecular 'Severo Ochoa', CSIC/Universidad Autónoma de Madrid, [1]Departamento de Morfología, Facultad de Medicina, Universidad Autónoma de Madrid, 28049 Madrid, Spain and [2]Center for Neurobiology and Behavior, Columbia University, New York, NY, USA

[3]Corresponding author
e-mail: javila@cbm.uam.es

J.J.Lucas and F.Hernández contributed equally to this work

Glycogen synthase kinase-3β (GSK-3β) has been postulated to mediate Alzheimer's disease tau hyperphosphorylation, β-amyloid-induced neurotoxicity and presenilin-1 mutation pathogenic effects. By using the tet-regulated system we have produced conditional transgenic mice overexpressing GSK-3β in the brain during adulthood while avoiding perinatal lethality due to embryonic transgene expression. These mice show decreased levels of nuclear β-catenin and hyperphosphorylation of tau in hippocampal neurons, the latter resulting in pretangle-like somatodendritic localization of tau. Neurons displaying somatodendritic localization of tau often show abnormal morphologies and detachment from the surrounding neuropil. Reactive astrocytosis and microgliosis were also indicative of neuronal stress and death. This was further confirmed by TUNEL and cleaved caspase-3 immunostaining of dentate gyrus granule cells. Our results demonstrate that *in vivo* overexpression of GSK-3β results in neurodegeneration and suggest that these mice can be used as an animal model to study the relevance of GSK-3β deregulation to the pathogenesis of Alzheimer's disease.

Keywords: Alzheimer's disease/β-catenin/conditional transgenic mice/GSK-3β/tau phosphorylation

Introduction

Alzheimer's disease (AD), the most common neurodegenerative disease in developed countries, is characterized by progressive memory loss and impairments in language and behavior that ultimately lead to death (Alzheimer, 1911; Yankner, 1996). The cognitive decline in AD is accompanied by neuronal atrophy and loss, mainly in the cortex, hippocampus and amygdala (Gomez-Isla *et al*., 1997). In addition to a specific pattern of neuronal cell death, AD is characterized by two neuropathological hallmarks, senile plaques and neurofibrillary tangles (NFTs). Senile plaques are extracellular deposits of amyloid fibrils composed of the 39–43 amino acid β-amyloid peptide (Aβ) often surrounded by dystrophic neurites (Masters *et al*., 1985; Selkoe, 1994). NFTs are intraneuronally generated aggregates of paired helical filaments (PHFs), which are assembled from hyperphosphorylated forms of the microtubule-associated protein tau (Grundke-Iqbal *et al*., 1986; Lee *et al*., 1991).

Molecular insights into AD pathogenesis have arisen from genetic studies in families affected by inherited forms of AD (FAD). These account for only a small percentage of AD cases but have allowed the identification of mutations in three different genes that are responsible for triggering the disease. These genes are the presenilins-1 and -2 (PS-1 and PS-2) and the amyloid precursor protein (APP) (Hardy, 1996). Mutations in APP result in increased production of Aβ (Price and Sisodia, 1998), while PS-1 and PS-2 mutations favor processing of APP into the long and most amyloidogenic form of Aβ ($A\beta_{42}$) (Duff *et al*., 1996; Price and Sisodia, 1998). This genetic evidence, together with *in vitro* and *in vivo* studies of Aβ-induced neurotoxicity, suggests that Aβ formation and/or aggregation is a key event in triggering AD. However, little is known about downstream intracellular effectors that account for neuronal dysfunction, although activation of glycogen synthase kinase-3 (GSK-3) has been proposed (see below).

GSK-3 is a proline-directed serine/threonine kinase that was originally identified as a result of its role in glycogen metabolism regulation, the CNS being the tissue with the highest GSK-3 levels (Woodgett, 1990). Apart from being implicated in insulin and insulin-like growth factor-1 (IGF-1)-mediated signal transduction, GSK-3 is also involved in the wnt/wingless signaling pathway as the key enzyme regulating β-catenin stability and, as a consequence, its translocation to the nucleus and its transcriptional activity (Barth *et al*., 1997; Anderton, 1999).

Two forms of GSK-3, referred to as GSK-3α and GSK-3β, each encoded by a distinct gene, have been identified (Woodgett, 1990). GSK-3β was found to be identical to tau protein kinase I (TPK I), an enzyme that was identified in brain extracts due to its ability to phosphorylate tau *in vitro* (Ishiguro *et al*., 1993). GSK-3β is one of the best candidate enzymes for generating the hyperphosphorylated tau that is characteristic of PHFs. GSK-3β has been shown to phosphorylate tau in most sites hyperphosphorylated in PHFs, both in transfected cells (Lovestone *et al*., 1994) and *in vivo* (Hong *et al*., 1997; Munoz-Montano *et al*., 1997). Furthermore, GSK-3β accumulates in the cytoplasm of pretangle neurons and its distribution in brains staged for AD neurofibrillary changes is coincident with the sequence of development of these changes (Shiurba *et al*., 1996; Pei *et al*., 1999).

Exposure of cortical and hippocampal primary neuronal cultures to Aβ has been shown to induce activation of GSK-3β (Takashima *et al*., 1996), tau hyperphosphoryl-

© European Molecular Biology Organization

ation (Busciglio *et al*., 1995; Ferreira *et al*., 1997) and cell death (Takashima *et al*., 1993; Busciglio *et al*., 1995). Blockade of GSK-3β expression or activity, either by antisense oligonucleotides or by lithium, prevents Aβ-induced neurodegeneration of cortical and hippocampal primary cultures (Takashima *et al*., 1993; Alvarez *et al*., 1999).

PS-1 has been shown to directly bind GSK-3β and tau in co-immunoprecipitation experiments from human brain samples (Takashima *et al*., 1998). Thus, the ability of PS-1 to bring GSK-3β and tau into close proximity suggests that PS-1 may regulate phosphorylation of tau by GSK-3β. Mutant forms of PS-1 in transfection experiments result in increased PS-1/GSK-3β association and increased phosphorylation of tau (Takashima *et al*., 1998). Furthermore, PS-1 has also been shown to form a complex with the GSK-3β substrate β-catenin in transfected cells (Murayama *et al*., 1998; Yu *et al*., 1998) and *in vivo* (Yu *et al*., 1998; Zhang *et al*., 1998), and this interaction increases β-catenin stability (Zhang *et al*., 1998). Pathogenic PS-1 mutations reduce the ability of PS-1 to stabilize β-catenin, which in turn results in decreased β-catenin levels in AD patients with PS-1 mutations (Zhang *et al*., 1998).

In view of the evidence linking GSK-3β with PHF tau phosphorylation, Aβ-induced neurotoxicity, PS-1 mutations and β-catenin stability, we reasoned that deregulation of GSK-3β in the brain might be a key aspect of AD pathogenesis. To test this, we have created transgenic mice overexpressing GSK-3β in the forebrain in a regulatable manner using the tet system. Here we show that overexpression of GSK-3β in the cortex and hippocampus leads to decreased levels of nuclear β-catenin, increased phosphorylation of tau in AD relevant epitopes, neuronal cell death and reactive astrocytosis and microgliosis.

Results

Mouse design

The tet-regulated system has been used for conditional gene expression in eukaryotic cell systems and mice (Gingrich and Roder, 1998). By using this system to drive transgenic expression of a mutated form of huntingtin, we have recently generated the first conditional animal model of a neurodegenerative disease (Yamamoto *et al*., 2000). The tet-regulated system can be particularly useful when mimicking adulthood pathological conditions since it may be used to circumvent perinatal lethality due to toxicity of the transgene (Yamamoto *et al*., 2000). Since GSK-3β overexpression has been postulated to be embryonic lethal (Brownlees *et al*., 1997), we decided to use the tet-regulated system to generate transgenic mice overexpressing GSK-3β.

Regulation of the system is achieved through the tetracycline-regulated transactivator (tTA), a chimeric protein comprised of the tet-repressor DNA-binding domain and the transactivation domain of viral protein VP16 of herpes simplex virus (Gossen and Bujard, 1992). This protein binds specifically to the tetO operator sequence and induces transcription from an adjacent cytomegalovirus (CMV) minimal promoter. The combination of both tTA and the tetO elements thus allows for continual transactivation of a given transgene. Tetracycline and its analogs can bind to tTA. When this happens, tTA is prevented from binding to tetO, and transcription is inhibited.

We generated a plasmid (BitetO) carrying the bi-directional tet-responsive promoter (Baron *et al*., 1995) followed by both a GSK-3β cDNA (encoding a myc epitope at its 5′ terminus) in one direction and, in the other direction, a cDNA encoding β-galactosidase (β-gal) fused to a nuclear localization signal (Figure 1A). The resultant plasmid was assayed in transfection experiments performed in COS cells (Figure 1B). This plasmid, by itself or cotransfected with an expression vector coding for tau (Figure 1B, lanes 1 and 2), had no effect on GSK-3β levels as shown by western blotting with an antibody against GSK-3β. When cotransfected with a plasmid that allows expression of tTA (Figure 1B, lanes 3 and 4) a marked increase in GSK-3β levels was evident. This resulted in increased phosphorylation of tau as demonstrated by western blotting with the PHF-1 antibody that recognizes a PHF tau phosphorylation epitope. When tetracycline was present (Figure 1B, lanes 5 and 6), transactivation of GSK-3β was abolished. These experiments therefore demonstrate conditional expression of GSK-3β from the BitetO construct (Figure 1A).

The BitetO construct was then microinjected into oocytes and the five resulting transgenic mouse lines were generically designated TetO (Figure 1C). In the tTA mouse lines, the tTA transgene is under the control of the calcium/calmodulin kinase IIα promoter (CamKIIα–tTA lines E and B) (Mayford *et al*., 1996). These tTA lines were chosen to allow for restricted, conditional expression in the CNS, with particularly high expression in the forebrain (Mayford *et al*., 1996; Yamamoto *et al*., 2000). When the TetO mice are crossed with tTA mice, the resulting double transgenic progeny (designated Tet/GSK-3β) are expected to constitutively express both transgenes (Figure 1C). This expression, however, can be abolished in the presence of tetracycline or its analogs.

Characterization of the different Tet/GSK-3β mouse lines

Our previous experience in generating conditional transgenic mice with the tet-regulated system indicates that the genomic site of insertion and/or copy number of the tetO construct influences the final pattern and level of transactivation by tTA. The β-Gal reporter sequence in the BitetO construct permits quick analysis of the pattern of transgene expression in the double transgenic mice either by X-Gal staining or by immunohistochemistry against β-Gal, and furthermore, allows for testing the efficacy of transgene silencing by tetracycline. We took advantage of this to decide which TetO mouse lines were more suitable for our study.

When the five TetO lines were bred with tTA lines, three of them showed β-Gal expression only in the striatum (data not shown). The two remaining TetO lines (lines G6 and G7) transactivate β-Gal in a spatial pattern very similar to that of endogenous CamKIIα, with expression evident in the cortex, hippocampus, striatum and amygdala (Figure 2). These two lines were especially suitable for our study since they exhibited high levels of transgene expression in brain regions relevant to AD such as the cortex and hippocampus, and we have therefore

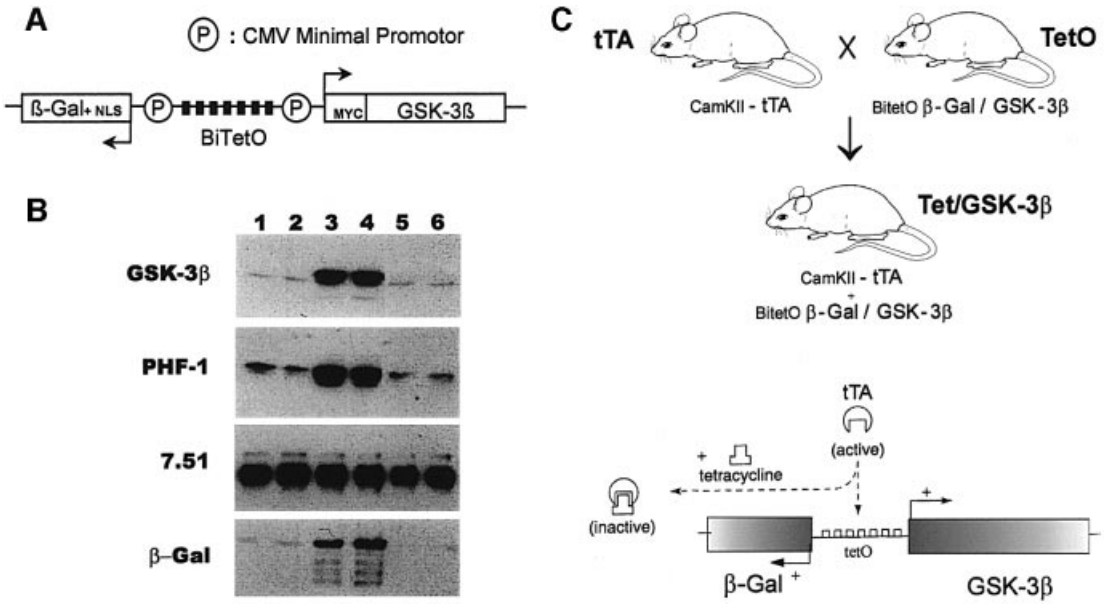

Fig. 1. Mouse design. (**A**) Schematic representation of the BitetO construct. This consists of seven copies of the palindromic tet operator sequence flanked by two CMV promoter sequences in divergent orientations. This bi-directional promoter is followed by a GSK-3β cDNA sequence (encoding a myc epitope at its 5′-end) in one direction and β-galactosidase (LacZ) sequence including a nuclear localization signal (NLS) in the other. (**B**) COS cells were co-transfected with the plasmid containing the BitetO construct and an expression vector coding for human tau (lanes 1–6), a third plasmid that allows expression of tTA was added (lanes 3–6) either in the absence (lanes 3 and 4) or in the presence (lanes 5 and 6) of 1 μg/ml tetracycline in the culture medium. Protein extracts were probed with antibodies against GSK-3β, AD-like phosphorylated tau (PHF-1), total tau (7.51) and β-galactosidase (β-Gal). (**C**) Tet/GSK-3β mice are generated by crossing mice expressing tTA under control of the CamKIIα promoter (tTA) with mice that have incorporated the BitetO construct in their genome (TetO). The double transgenic progeny (Tet/GSK-3β) are expected to express GSK-3β constitutively in the brain unless tetracycline or analogs are given orally thus preventing transactivation by tTA.

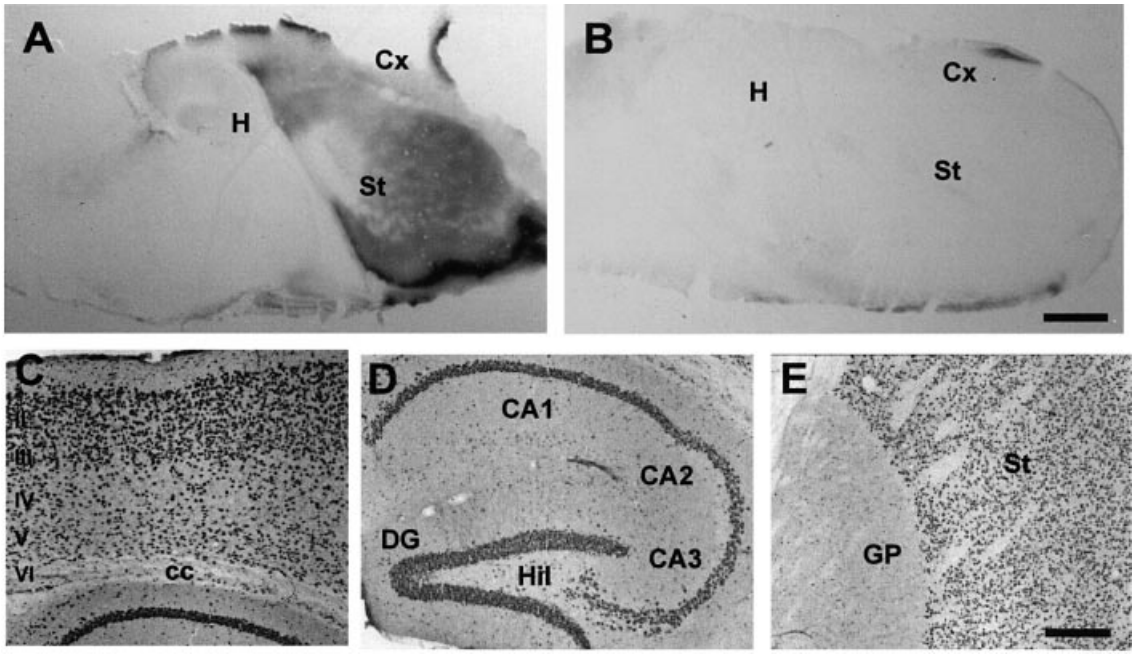

Fig. 2. Pattern of transgene expression in Tet/GSK-3β mice. (A and B) X-gal staining of brain sagittal sections from P0 Tet/GSK-3β mice that were either drug-naive (**A**) or born after giving doxycycline to the mother for 5 days immediately prior to birth (**B**). (C–E) β-galactosidase immunohistochemistry in sagittal sections of adult (3 months) Tet/GSK-3β mouse brain reveals expression in the different neuronal layers of the cortex (**C**), the hippocampus (**D**) and the striatum (**E**). H, hippocampus; Cx, cortex; St, striatum; II–VI, cortical layers; cc, corpus callosum; DG, dentate gyrus; Hil, hillus; GP, globus pallidus. Scale bar in (B) corresponds to 1 mm in (A) and (B). Scale bar in (E) corresponds to 200 μm in (C–E).

focused the rest of the study on lines G6 and G7. Immunohistochemistry in brain sections of adult Tet/GSK-3β mice shows β-Gal expression in the different neuronal layers of the cortex, the different fields of the hippocampus (including subiculum, CA1, CA2, CA3 and dentate gyrus), and in the striatum (Figure 2C–E). No

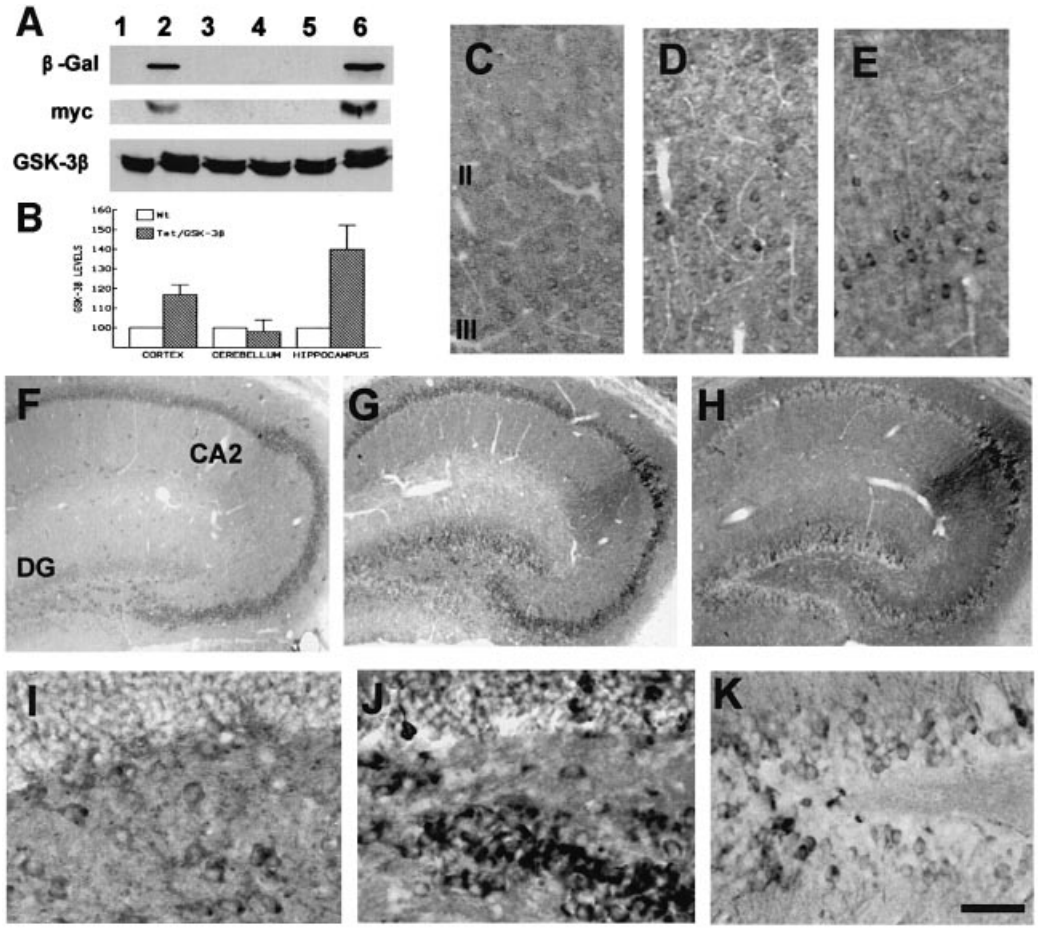

Fig. 3. Overexpression of GSK-3β in the cortex and hippocampus of Tet/GSK-3β mice. (**A**) Western blot of protein extracts from cortex (lanes 1 and 2), cerebellum (lanes 3 and 4), and hippocampus (lanes 5 and 6) of wild-type (lanes 1, 3 and 5) or Tet/GSK-3β (lanes 2, 4 and 6) mice. (**B**) Histogram showing percent increase of GSK-3β levels in Tet/GSK-3β mice. (**C–E**) Immunohistochemistry in cortical sections of wild-type (C) or Tet/GSK-3β (D and E) mice; performed with antibodies against GSK-3β (C and D) or myc (E). (**F–H**) Immunohistochemistry in hippocampal sections of wild-type (F) or Tet/GSK-3β (G and H) mice; performed with an antibody against GSK-3β (F and G) or myc (H). (**I–K**) High power magnification of the dentate gyri shown in (F–H). Scale bar corresponds to 100 μm in (C–E), 200 μm in (F–H), 60 μm in (I) and (J), and 40 μm in (K).

β-Gal expression was detected in other brain regions such as globus pallidus, thalamus, brainstem and cerebellum (Figures 2A, E and 3A, and not shown). A similar pattern and level of transgenic expression was obtained when either CamKIIα–tTA line (E or B) was combined with one TetO line (G6 or G7). In this study we have used each combination interchangeably and thus henceforth we will use the terms tTA and TetO for single transgenic mice, and Tet/GSK-3β for the double transgenic animals.

Tet/GSK-3β mice were viable and fertile and appeared normal without pharmacological intervention to suppress transgene expression. This seemed to contradict the previously postulated toxicity of increased GSK-3β expression in brain (Brownlees *et al.*, 1997). However, heterozygote crosses between tTA and TetO mice did not yield the expected frequency of 25% for each genotype (wild type, tTA, TetO and Tet/GSK-3β). The Tet/GSK-3β mice were underrepresented (14%, $n = 401$). This might be indicative of lethality due to embryonic overexpression of GSK-3β in Tet/GSK-3β mice. We had previously observed perinatal transgene expression and lethality in our CamKIIα–tTA-driven animal model of Huntington's disease (HD94) (Yamamoto *et al.*, 2000). In the case of HD94 mice, if pregnant mice are given the tetracycline analog doxycycline (2 mg/ml) in drinking water *ad libitum* from E15 to birth, only postnatal transgenic expression takes place and the frequency of the four expected genotypes is restored to 25%. We thus decided to apply the same program of perinatal doxycycline treatment to the Tet/GSK-3β mice. We found that at P0, non-treated mice show X-gal staining in the forebrain while staining was absent in treated mice (Figure 2A and B). This demonstrates that transgene expression in Tet/GSK-3β mice begins during embryonic life and that it can be inhibited with doxycycline. As expected, prenatal doxycycline treatment normalized to 25% the frequency of Tet/GSK-3β mice and thus, to maximize yield of double transgenic mice in litters, the perinatal doxycycline treatment was generally employed.

Tet/GSK-3β mice overexpress GSK-3β in the cortex and hippocampus

Western blot analysis was used to confirm that the brain regions which show β-Gal expression also display increased levels of GSK-3β. Probing protein extracts with an anti-myc antibody demonstrated that the highest

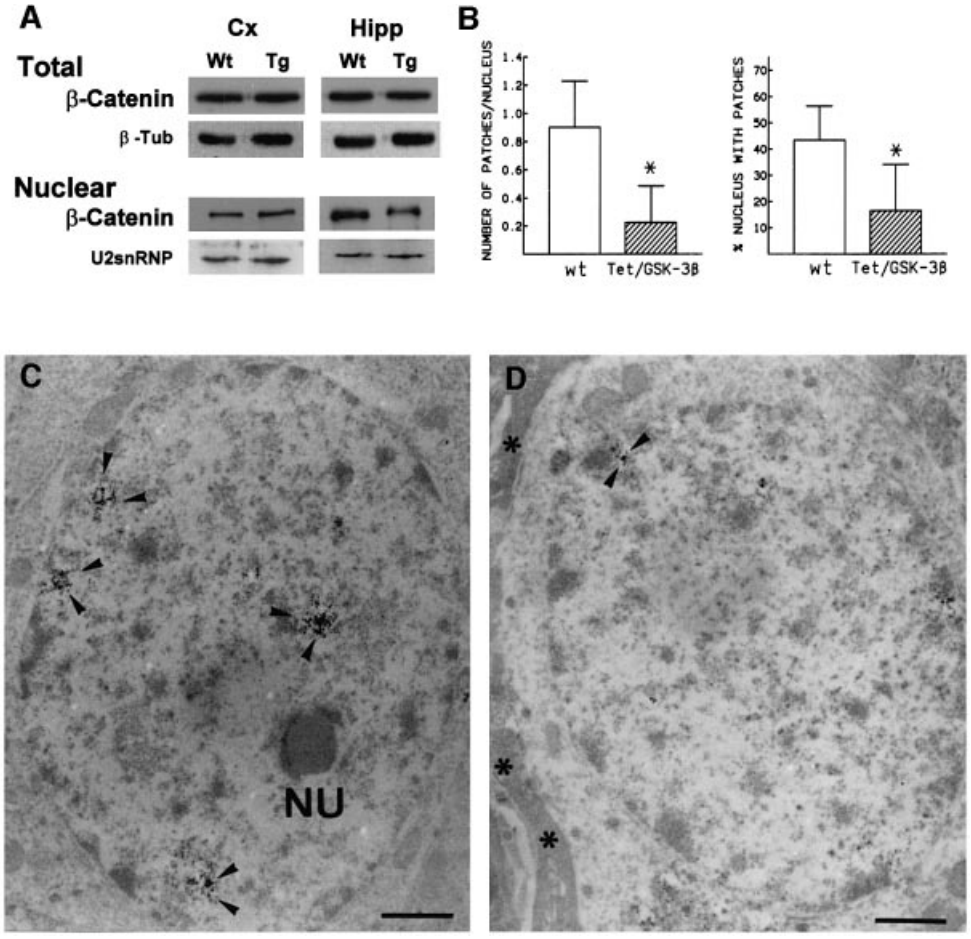

Fig. 4. Effect of GSK-3β overexpression on β-catenin levels. (**A**) Representative western blot of total cellular and nuclear preparations from the cortex (Cx) and hippocampus (Hipp) of wild-type (Wt) or Tet/GSK-3β (Tg) mice probed with anti-β-catenin antibody. β-tubulin and U2snRNP blots are shown as controls of total and nuclear protein loading. (**B**) Quantification of patches of β-catenin in the nucleus of dentate gyrus granule cells from wild-type and Tet/GSK-3β mice as detected by immunoelectron microscopy. (**C**) Electron microscopy photomicrograph showing a dentate gyrus neuron from a wild-type mouse with several patches of β-catenin reaction product (arrowheads). NU, nucleolus. (**D**) Electron microscopy photomicrograph showing a dentate gyrus neuron from a Tet/GSK-3β mouse. Asterisks, astrocitic process. No heavy metal staining was performed. Scale bars in (C) and (D) correspond to 0.1 μm.

level of transgenic GSK-3β expression takes place in the hippocampus, followed by the cortex (Figure 3A), while little expression could be detected in the striatum (not shown). Accordingly, probing extracts from 3-month-old mice with an antibody raised against GSK-3β (Figure 3A and B) we observed a significant ($p < 0.02$) 40 ± 12.4% increase in GSK-3β levels in the hippocampus of Tet/GSK-3β mice with respect to wild-type mice. Cortical extracts also showed increased (17 ± 5%) levels of GSK-3β in Tet/GSK-3β mice. No differences in GSK-3β levels were found in the striatum (not shown) or in non-forebrain regions such as cerebellum (Figure 3B).

To gain insight into which cell populations are overexpressing GSK-3β, we performed immunohistochemistry with both anti-myc and anti-GSK-3β antibodies. In the cortex, increased immunoreactivity (IR) for GSK-3β was restricted to layer II and III pyramidal neurons of the frontal cortex (Figure 3C–E) and to lamina VI neurons adjacent to the corpus callosum (not shown).

In the hippocampus, overexpression of GSK-3β was most evident in dentate gyrus and CA2 neurons (Figure 3F–H). The dentate gyrus of wild-type mice showed very weak IR for GSK-3β (Figure 3F and I), while almost every neuron in the dentate gyrus of Tet/GSK-3β mice showed strong immunostaining with both anti-GSK-3β and anti-myc antibodies (Figure 3J and K). Interestingly, neurons with remarkably high staining often exhibited abnormal morphologies such as shrunk cell bodies (Figure 3J). In CA2 pyramidal neurons, a prominent staining in both cell bodies and dendrites was seen in Tet/GSK-3β mice (Figure 3G–H).

Nuclear β-catenin destabilization and tau hyperphosphorylation in Tet/GSK-3β mice

We next analyzed by western blotting the effect of GSK-3β overexpression on its AD-related substrates β-catenin and tau. β-catenin is a component of cell–cell adherent junctions but also associates with high-mobility-group (HMG)-box transcription factors of the T-cell factor and lymphoid enhancer factor (Tcf/LEF) family and promotes transcription of target genes. GSK-3 activity is key in regulating β-catenin stabilization and subsequent nuclear translocation (Barth *et al*., 1997; Anderton, 1999).

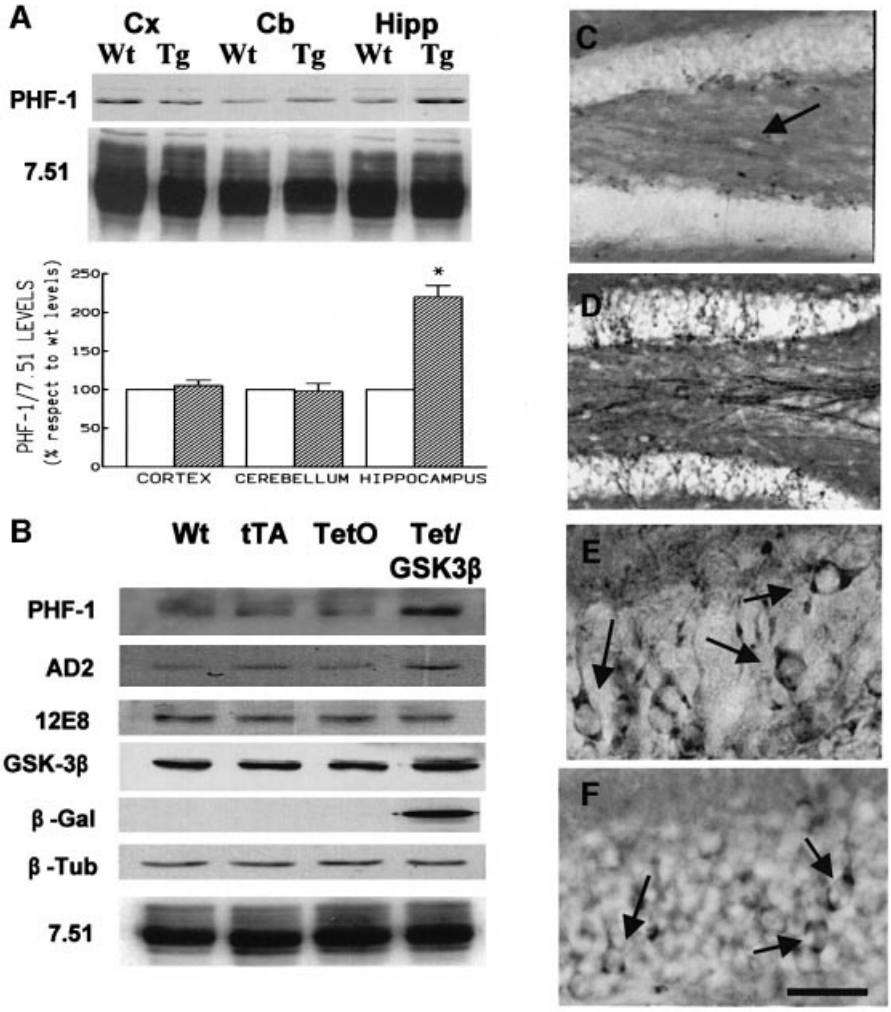

Fig. 5. Hyperphosphorylation and somatodendritic localization of tau in Tet/GSK-3β mice. (**A**) Western blot of protein extracts from cortex (Cx), cerebellum (Cb) and hippocampus (Hipp) of wild-type (Wt) or Tet/GSK-3β (Tg) mice probed with PHF-1 and 7.51 antibodies. Histogram shows the percentage of PHF-1/total (as demonstrated with 7.51 antibody) tau in Tet/GSK-3β mice with respect to wild-type mice. Note the significant increase in hippocampus ($p < 0.05$). (**B**) Western blot of hippocampal extracts from wild-type (Wt), tTA, TetO or Tet/GSK-3β mice probed with the indicated antibodies. (**C**–**E**) PHF-1 immunohistochemistry in the dentate gyrus of wild-type (C) or Tet/GSK-3β (D and E) mice. (**F**) Immunohistochemistry performed with 7.51 antibody in the dentate gyrus of a Tet/GSK-3β mouse. The arrow in (C) indicates faintly stained mossy fibers. The scale bar corresponds to 200 μm in (C) and (D), and 60 μm in (E) and (F).

We first analyzed the levels of β-catenin in total cortical and hippocampal extracts (Figure 4A). No differences were found between wild-type and Tet/GSK-3β mice. However, when we analyzed β-catenin levels in different cellular compartments (nucleus, cytosol and membrane), we observed a significant ($p < 0.05$, $n = 6$) $35 \pm 8\%$ reduction in nuclear β-catenin levels in the hippocampus of Tet/GSK-3β mice compared with wild-type littermates (Figure 4A). The reason why we do not find a decrease in nuclear β-catenin content in the cortex is most likely to be due to the reduced number of cortical neurons that show transgenic GSK-3β expression (see Figure 3).

A recent study has shown that immunoelectron microscopy can be used to study changes in levels and compartmentalization of β-catenin (Eger *et al.*, 2000). These authors found that cytoplasmic β-catenin has a diffuse and uniform distribution in mesenchymal cells. In contrast, nuclear β-catenin is found in discrete spot-like structures that can be quantified by immunoelectron microscopy. We have analyzed by immunoelectron microscopy the granule cells of the dentate gyrus and found the same spot-like pattern of nuclear β-catenin. Figure 4C shows a granule neuron from a wild-type mouse with several patches of β-catenin reaction product. Interestingly, the decrease in nuclear β-catenin found by western blotting in Tet/GSK-3β mice was also evident by this technique (Figure 4B–D). Quantification of these patches of nuclear β-catenin in wild-type and Tet/GSK-3β mice revealed a 75% reduction ($p < 0.0001$) in the number of β-catenin patches per nucleus in Tet/GSK-3β mice.

We next performed western blotting with the phospho-tau antibody PHF-1 in those brain regions that show myc expression (cortex, striatum and hippocampus) as well as in the cerebellum. Increased levels of tau phosphorylation were found in hippocampus (Figure 5A). The increase in AD-like phosphorylation of tau detected with the PHF-1 antibody was reproduced using the AD2 antibody raised against the same phosphoepitope of tau (Figure 5B). The

increase in PHF-1 and AD2 IR in Tet/GSK-3β mice is not due to altered levels of total tau since no increase was observed with the phosphorylation-independent tau antibody 7.51 that recognizes all tau isoforms. Furthermore, phosphorylation at serine 262, which is not adjacent to a proline residue and which has been shown to be independent of GSK-3β *in vivo* (Munoz-Montano *et al*., 1997), is not affected in Tet/GSK-3β mice as detected by the 12E8 antibody (Figure 5B).

We compared tau phosphorylation and transgenic protein expression in the four possible genotypes (wild type, tTA, TetO and Tet/GSK-3β) (Figure 5B). Only Tet/GSK-3β mice showed β-Gal expression and increased levels of GSK-3β, PHF-1 and AD2 tau, therefore demonstrating that transgenic expression and subsequent effects in Tet/GSK-3β mice were due to transactivation by tTA of the BitetO construct and not due to leakage of the latter in the TetO mice.

Somatodendritic localization of AD-like hyperphosphorylated tau

We analyzed by immunohistochemistry which hippocampal neuronal populations exhibit the increase in PHF-1 IR observed by western blotting. Increased PHF-1 immunostaining was most evident in the dentate gyrus (Figure 5C–E). In wild-type mice, granule cells of the dentate gyrus show no detectable PHF-1 IR (Figure 5C), although some staining could be detected in the mossy fibers projecting to CA3 (Figure 5C). Tet/GSK-3β mice show a marked increase in the staining of mossy fibers (Figure 5D) and, interestingly, most granule cells show strong somatodendritic PHF-1 immunostaining, thus resembling the pretangle stage of AD neurofibrillary degeneration (Figure 5D and E).

Phosphorylation of tau by GSK-3β decreases the affinity of tau for microtubules *in vitro* and in transfected cells (Lovestone *et al*., 1996). This may explain in part the somatodendritic staining found with the PHF-1 antibody. To test this, we performed immunohistochemistry with 7.51, an antibody raised against the tubulin-binding domain of tau and that therefore recognizes tau only when it is not bound to microtubules. Interestingly, the 7.51 antibody stained somas of Tet/GSK-3β but not wild-type dentate gyrus granule cells (Figure 5F). The morphology of 7.51 stained cells was very similar to that observed with PHF-1 antibody (Figure 5E).

Strong somatodendritic immunostaining of hyperphosphorylated tau may also be indicative of aberrant aggregated forms of tau such as PHFs. Thioflavine-S staining in AD brains reveals both neurofibrillary tangles and amyloid plaques. We therefore performed Thioflavine-S staining in brain sections of Tet/GSK-3β mice. No Thioflavine-S fluorescence was detected, either in the granule cells of the dentate gyrus or in any other brain region, indicating the absence of PHF bundles and of β-sheet protein aggregates.

The lack of Thioflavine-S fluorescence could still be compatible with the existence of few, short PHFs, thus representing initial steps of neurofibrillary degeneration. To analyze this possibility, we then studied Tet/GSK-3β granule cells by electron microscopy since they show strong somatodendritic immunolabeling for PHF-1. A diffuse reaction product was present in the perikaryon of these neurons (Figure 6), although in some cases we also observed patches of dark reaction product (Figure 6C). However, PHFs were not observed either in the dark reaction product patches or in other portions of the diffuse immunolabeled cytoplasm. Interestingly, immunolabeled material was often seen along the cytoplasmic face of the rough endoplasmic reticulum (RER) cisternae, and the above mentioned dark stained patches were, on some occasions, in close proximity to these labeled RER cisternae (Figure 6C). Interestingly, Tet/GSK-3β neurons with diffuse PHF-1 cytoplasmic labeling very frequently appeared detached from the surrounding neuropil, showing a widened extracellular space along most of their periphery (Figure 6A) whereas unlabeled neurons did not show any detachment. We also observed no detachment of granule cell neurons of wild-type mice.

Neuronal cell death and reactive gliosis in the hippocampus of Tet/GSK-3β mice

Previous studies have demonstrated that GSK-3β is inhibited by the phosphatidylinositol 3-kinase/protein kinase B survival pathway that prevents apoptosis (Pap and Cooper, 1998; Hetman *et al*., 2000). This, together with the observation that destabilization of β-catenin by mutations in PS-1 potentate neuronal apoptosis (Zhang *et al*., 1998), prompted us to explore whether apoptosis was taking place in Tet/GSK-3β mice as a consequence of the overexpression of GSK-3β.

We compared TUNEL staining in wild-type and Tet/GSK-3β mice. Similar to tau phosphorylation and β-catenin destabilization, increased TUNEL was found in the hippocampus of Tet/GSK-3β mice. Dentate gyrus granule cells of Tet/GSK-3β mice showed a marked and significant ($p < 0.0005$) increase in TUNEL staining as shown in Figure 7A–C (up to 5 labeled granule cells per 30 μm section of Tet/GSK-3β dentate gyrus versus virtually no labeling in wild-type dentate gyrus). We then analyzed whether dentate gyrus granule cells showed indications of apoptosis other than DNA fragmentation as shown by TUNEL. Interestingly, a concomitant immunoreactivity against cleaved caspase-3 was found in granule cell neurons of Tet/GSK-3β mice (Figure 7D), while no labeling was detected in wild-type mice (not shown).

We next tested whether the neuronal alterations and/or death triggered by overexpression of GSK-3β in Tet/GSK-3β mice were accompanied by glial alterations such as reactive astrocytosis and microgliosis. Immunohistochemistry performed with an antibody raised against glial fibrillary acidic protein (GFAP) revealed reactive astrocytosis in the dentate gyrus of Tet/GSK-3β mice (Figure 7C, E and F). Electron microscopy studies confirmed the presence of highly activated astrocytic processes, full of glial intermediate filaments, in the dentate gyrus of Tet/GSK-3β mice (Figures 4D and 7G). These were often found surrounding PHF-1 IR neurons (Figure 7G).

To test whether microgliosis was taking place in the hippocampus of Tet/GSK-3β mice we performed immunohistochemistry with OX42, LN-3 and ED1 antibodies. Similar results were obtained with all of these three antibodies (Figure 7H shows OX-42 immunohistochemistry). When compared with wild-type hippocampal sections, an increase in fine microglial processes was found in the stratum granulare of Tet/GSK-3β mice.

Furthermore, immunostained cell bodies corresponding to reactive microglia were found only in Tet/GSK-3β mice, mainly in the stratum moleculare of the hippocampus (arrowheads in Figure 7H).

Discussion

By using a conditional transgenic approach here we show that *in vivo* overexpression of GSK-3β results in

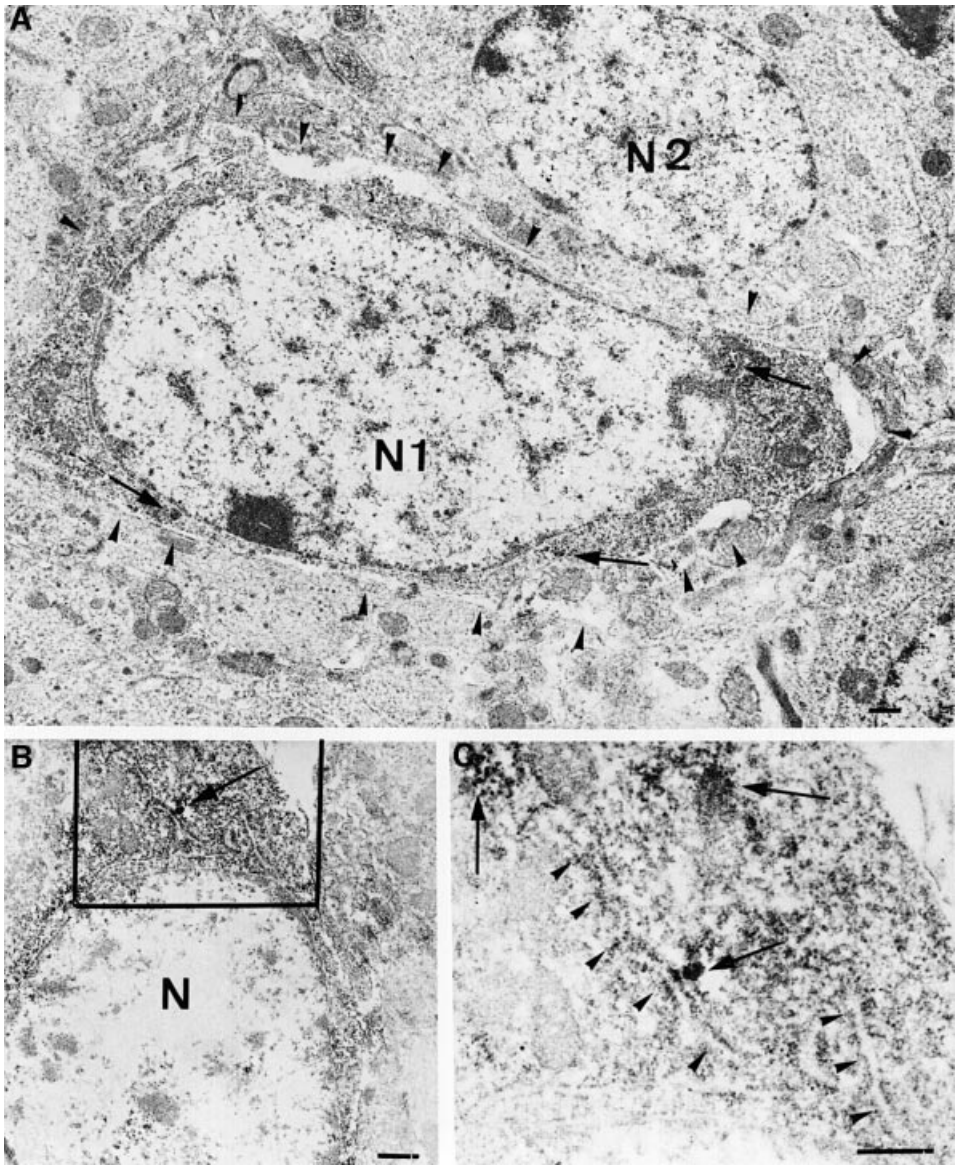

Fig. 6. Electron microscopy study of PHF-1 positive neurons. (**A**) Electron micrograph of two neurons from the dentate gyrus of Tet/GSK-3β mouse hippocampus. N1, nucleus of a PHF-1 immunopositive neuron exhibiting most of its perimeter detached from the surrounding neuropil (arrowheads), in addition to diffuse cytoplasmic immunostaining. N2, nucleus of a PHF-1 immunonegative neuron. (**B**) Another PHF-1 immunopositive neuron from the dentate gyrus of the same mouse as in (A), showing PHF-1 reaction product in patches and associated with RER. N, unlabeled nucleus. (**C**) high magnification of the framed portion in (B), showing the patches of reaction product (arrows) and the labeling of the RER (arrowheads). No heavy metal staining was performed. Calibration bar corresponds to 0.5 μm in all panels.

Fig. 7. Neuronal death and reactive gliosis in Tet/GSK-3β mice. (A and B) TUNEL staining of the dentate gyrus of wild-type (**A**) or Tet/GSK-3β (**B**) mice. Arrows indicate TUNEL positive nuclei. (**C**) Histograms showing the number of TUNEL positive neurons and of GFAP IR cells per 30 μm sagittal section of the dentate gyrus from mice of the four genotypes: wild-type, tTA, Tet-O and Tet/GSK-3β. Note the significant increases in Tet/GSK-3β mice with respect to wild type (*, $p < 0.0005$). (**D**) Immunohistochemistry against cleaved caspase-3 in the dentate gyrus of a Tet/GSK-3β mouse. (E and F) GFAP immunohistochemistry in the dentate gyrus of wild-type (**E**) or Tet/GSK-3β (**F**) mice. (**G**) Electron micrograph of the dentate gyrus of Tet/GSK-3β mouse hippocampus showing a hypertrophied astrocytic process (black star) adjacent to a PHF-1 immunostained neuron. N, nucleus. Asterisk, diffuse cytoplasmic PHF-1 immunostaining. Inset, high magnification of the astrocytic process showing characteristic bundles of glial intermediate filaments. (**H**) OX-42 immunostaining of the dentate gyrus of a Tet/GSK-3β mouse. Arrows indicate fine immunoreactive microglial processes. Arrowheads indicate immunostained reactive cell bodies. SM, stratum moleculare; SG, stratum granulare; H, hillus. Scale bars correspond to 50 μm in (A), (B) and (D); 60 μm in (E) and (F); 0.5 μm in (G); and 30 μm in (H).

neurodegeneration. Conditional transgenic mice overexpressing GSK-3β also mimic different biochemical and cellular aspects of AD, such as β-catenin destabilization and pretangle-like somatodendritic localization of hyperphosphorylated tau. Our results therefore support the hypothesis that deregulation of GSK-3β might be a critical

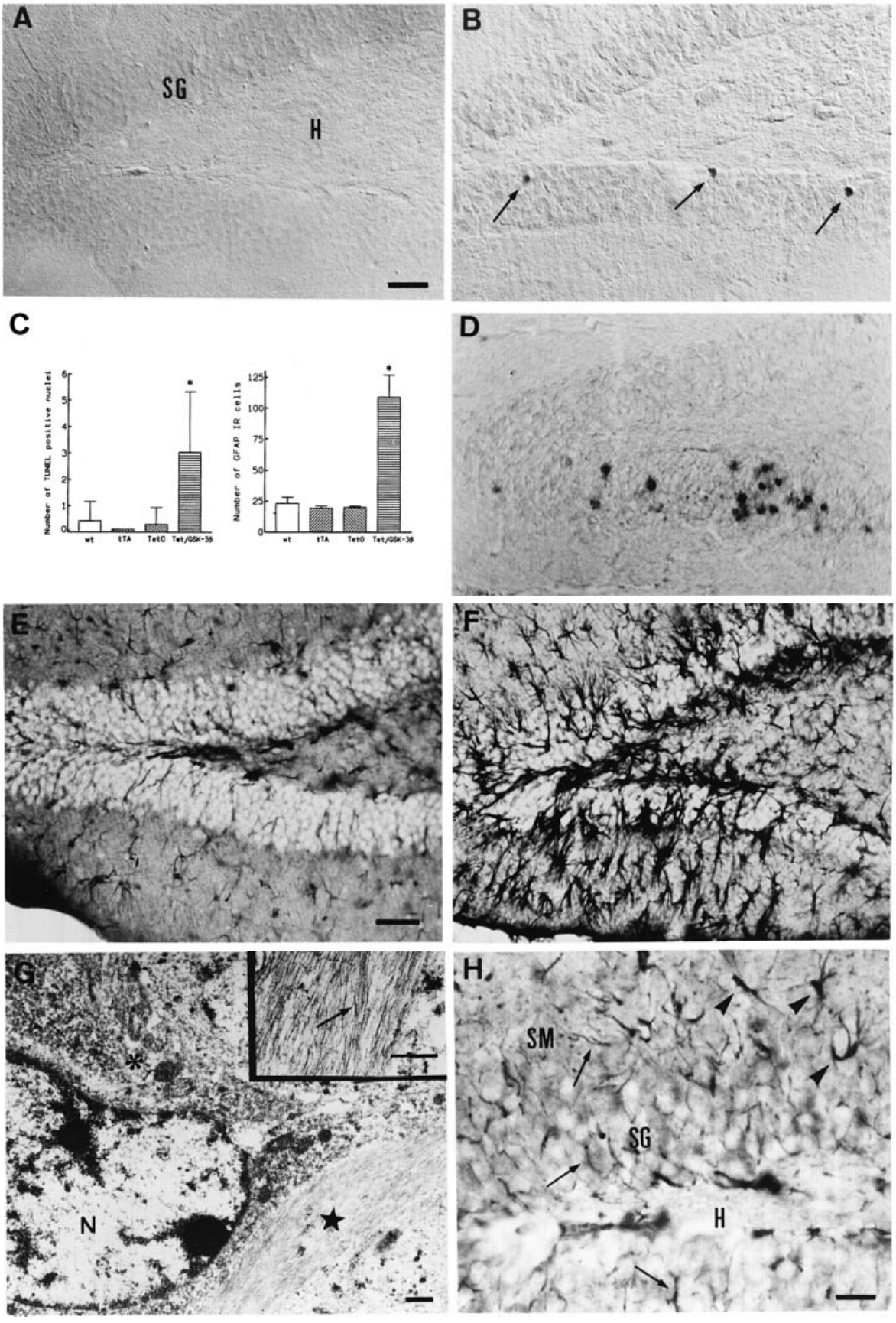

event in the pathogenesis of AD and raise the possibility that these mice may serve as a useful animal model to study some aspects of this pathology.

GSK-3β is active during animal development as a component of the Wnt signaling pathway and plays an important role in cell-fate decisions and pattern formation (Miller and Moon, 1996). Accordingly, the ability of lithium to inhibit GSK-3β has been suggested to account for its teratogenic effects (Klein and Melton, 1996; Stambolic *et al*., 1996), and that GSK-3β knockout mice die during embryonic life (Hoeflich *et al*., 2000). Apart from their well-established roles in early development, Wnt signaling and GSK-3β have been shown to participate in postnatal cerebellar granule cell synaptogenesis (Lucas and Salinas, 1997; Hall *et al*., 2000). Toxicity of GSK-3β overexpression during embryonic and postnatal development of the CNS may explain why Brownlees and collaborators were unable to generate transgenic mice with detectable overexpression of GSK-3β even with neuronal-specific promoters. This prompted these authors to suggest the use of tightly controlled inducible expression systems (Brownlees *et al*., 1997). In our case, we also find that a fraction of double transgenic mice die perinatally and that this can be rescued by silencing transgene expression during embryonic life. However, some mice can survive without pharmacological intervention. There are at least two reasons why this may happen. First, the promoter that we use (CamKIIα) has a more restricted pattern of expression than the one employed by Brownlees and collaborators (neurofilament-light chain). Secondly, in our binary system the transgene by itself is silent. This avoids lethality of founders due to the toxicity of the transgene. Subsequent breeding with tTA mice allows us to select those double transgenic descendants with a genetic background permissive for the embryonic overexpression of the transgene.

Regarding the pattern of transgene expression driven by the CamKIIα promoter, there is a discrepancy between the widespread and strong expression of β-Gal in the cortex and hippocampus and the limited overexpression of GSK-3β in certain cortical and hippocampal neuronal subpopulations. Our results suggest that there must be a regulation of GSK-3β degradation depending on GSK-3 levels. This regulation is probably not equally efficient in all cell types, and dentate gyrus and CA2 seem to be the only hippocampal cell types that allow a detectable overexpression of GSK-3β as a consequence of increased transcription.

Somatodendritic accumulation of hyperphosphorylated tau is an early event in the evolution of AD neurofibrillary degeneration (Braak *et al*., 1994). Pretangle-like immunostaining of tau is found in transgenic mice overexpressing different isoforms of tau (Gotz *et al*., 1995; Brion *et al*., 1999; Ishihara *et al*., 1999; Spittaels *et al*., 1999). Somatodendritic localization of tau in these mice might be due to saturation of the tau binding capacity of microtubules. The excess tau is then susceptible to accumulate in the soma and undergo modifications such as phosphorylation and conformational changes. In Tet/GSK-3β mice, hyperphosphorylation and somatodendritic localization of tau take place without affecting the total level of tau, thus resembling more closely the situation found in AD and other taupathies. According to the increase in somatodendritic 7.51 immunostaining found in Tet/GSK-3β mice and to previous *in vitro* studies (Lovestone *et al*., 1996), increased tau phosphorylation in Tet/GSK-3β mice most likely leads to a decreased affinity of tau for microtubules and subsequent accumulation of the protein in the soma.

We find that somatodendritic tau in Tet/GSK-3β mice is often associated with the endoplasmic reticulum. Similar results were found in transgenic mice overexpressing the shortest isoform of tau (Brion *et al*., 1999) and in aged sheep (Nelson *et al*., 1993). In all of these cases, immunodetection was performed with antibodies that recognize phosphorylation or conformation epitopes found in PHF-tau. Interestingly, PHFs in AD brains are often found arising from the endoplasmic reticulum and other membrane structures (Gray *et al*., 1987; Metuzals *et al*., 1988; Papasozomenos, 1989). It is therefore possible that, in animal models, association of tau with the endoplasmic reticulum represents an early stage in the formation of neurofibrillary lesions. An additional and compatible explanation for the association of tau with the endoplasmic reticulum might be its interaction with PS-1. PS-1 has been found to bind both tau and GSK-3β in co-immunoprecipitation experiments performed on human brain extracts (Takashima *et al*., 1998), and PS-1 is located predominantly in the endoplasmic reticulum and in the Golgi apparatus (Selkoe, 1998).

Several mechanisms may account for the neuronal stress and death (revealed by reactive glia and TUNEL/cleaved caspase-3 staining) detected in Tet/GSK-3β mice. In view of the effects of GSK-3β overexpression on tau phosphorylation and compartmentalization, a possible mechanism could be the disorganization of the microtubule cytoskeleton. In this case, as a consequence of a diminished stabilization of microtubules by tau, a decrease in microtubule content similar to that found in AD brains (Terry, 1998) would be expected in Tet/GSK-3β mice. Additionally, GSK-3β is negatively regulated by the survival pathway involving PI-3 kinase, and challenging cultured cortical neurons with trophic factor withdrawal or with PI-3 kinase inhibitors leads to stimulation of GSK-3β that results in apoptosis (Pap and Cooper, 1998; Hetman *et al*., 2000). Finally, decreased β-catenin-mediated transcription has been shown to potentate neuronal apoptosis in primary neuronal cultures exposed to β-amyloid (Zhang *et al*., 1998) or transfected with mutant PS-1 (Weihl *et al*., 1999). Little is known about the target genes transactivated by β-catenin that are responsible for the increased susceptibility to apoptosis. Tet/GSK-3β mice can be a useful system to identify such genes by differential display or DNA-microarray approaches.

Substantial progress has been made during the last few years towards the generation of transgenic mouse models of AD, particularly in regard to the β-amyloid toxic cascade and plaque formation (Price and Sisodia, 1998). Sequential improvements have been achieved by generating mice with higher expression levels of mutated forms of APP and by breeding them with mutant PS-1 transgenic mice that favor APP processing into $A\beta_{42}$ (Guenette and Tanzi, 1999). However, if GSK-3β deregulation is a key event in the pathogenesis of AD, Tet/GSK-3β mice may constitute an alternative and/or complementary mouse model of AD. Most of the effort made to date in transgenic

models of AD has focused on mimicking the neuropathological hallmarks of AD. This may require excessively artificial modifications to reproduce within the life span of a mouse, something that is formed over many years in a human. Alternatively, it may simply not be possible to mimic all aspects of AD neuropathology in mice because it requires human-specific clues [as is the case for β-amyloid induced toxicity *in vivo* (Geula *et al*., 1998)]. GSK-3β is an enzyme found at the convergence of the pathways involved in AD-like tau hyperphosphorylation, β-amyloid-induced toxicity and PS-1 mutations. When compared with already existing mouse models of AD, Tet/GSK-3β mice are unique in the sense that they reproduce downstream intraneuronal dysfunction, which may be ultimately responsible for some aspects of AD. A prediction of this hypothesis would be that GSK-3β levels (or activity) and substrates should be found altered in AD patients. Evidence in favor of this has already been reported (Shiurba *et al*., 1996; Pei *et al*., 1999).

Neurodegeneration in Tet/GSK-3β mice is in good agreement with the neuroprotective effect of lithium, a relatively specific GSK-3β inhibitor. The neuroprotective effects of lithium have been ascribed to its ability to inhibit GSK-3β (Alvarez *et al*., 1999; Hetman *et al*., 2000) and to upregulate Bcl-2 and downregulate Bax proteins in neurons (reviewed in Manji *et al*., 1999). Tet/GSK-3β mice are thus a good tool to test the neuroprotective effect of forthcoming GSK-3β-specific inhibitors. Furthermore, their efficacy can be compared with the effect of silencing transgene expression by administering tetracycline analogs.

Materials and methods

Generation of injection fragment

An 8.0 kb *Ase*I fragment (BitetO) was used for microinjection. To generate BitetO, a 1.5 kb *Hin*dIII fragment corresponding to *Xenopus* GSK-3β cDNA with an N-terminal myc epitope was excised from a pcDNA3-GSK3 plasmid (S.Sanchez, L.Sayas, F.Lim, J.Diaz-Nido, J.Avila and F.Wandosell, submitted). This fragment was subcloned into the pCRII cloning vector (Invitrogen) digested with *Hin*dIII. The correct orientation was tested for by *Xho*I digestion. A 1.5 kb fragment was then excised by *Nsi*I–*Not*I digestion and subcloned into the *Pst*I–*Not*I sites of a plasmid containing a bidirectional tetO sequence flanked by CMV minimal promotors with lacZ reporter sequences (pBI-G, Clontech). Lastly, the 8.0 kb *Ase*I BitetO fragment was microinjected into single-cell CBAxC57BL/6 embryos. Founder mice were identified by PCR and confirmed by Southern analysis. Founder mice were then crossed with wild-type CBAxC57BL/6 mice and Southern analysis was performed on F_1 progeny to test for multiple insertion events of the microinjection fragment. All mice reported here resulted from a single integration event (data not shown).

COS cell transfections

COS-7 cells were maintained in Dulbecco's modified Eagle's medium (DMEM; Gibco-BRL) supplemented with 10% (v/v) fetal bovine serum, 2 mM glutamine, 100 U/ml penicillin and 100 μg/ml streptomycin, and incubated in 95% air/5% CO_2 in a humidified incubator at 37°C. Cells at 50–70% confluence in 35 mm diameters dishes were transiently transfected with LipofectAMINE (Gibco-BRL)/5 μg of DNA according to the manufacturer's recommendations. Cells were harvested and analyzed 48 h following transfection.

Animals

Mice were bred at the Centro de Biología Molecular 'Severo Ochoa' animal facility. Mice were housed four per cage with food and water available *ad libitum* and maintained in a temperature-controlled environment on a 12/12 h light–dark cycle with light onset at 07:00 h.

Antibodies

The following antibodies were kindly donated: 7.51 (Dr Wischik), PHF-1 (Dr Davies), 12E8 (Dr Seubert), AD2 (Dr Mourton-Gilles), OX42 (Dr Bovolenta) and U2snRNP (Dr Ortín). According to the residue numbering of the longest human tau isoform of 441 amino acids, antibody 12E8 reacts with tau when serine 262 is phosphorylated and antibodies PHF-1 and AD2 when serines 396 and 404 are phosphorylated. Sources of commercial antibodies against: GSK3β and β-catenin (Transduction Laboratories), β-tubulin (Sigma), β-galactosidase (Promega), myc (Developmental Studies Hybridoma Bank, IA), GFAP (PharMingen, CA), ED1 (Serotec, UK), cleaved caspase-3 (Cell Signaling Technology, MA).

Subcellular fractionation

To prepare membrane and cytosolic extracts, tissues were washed with ice-cold phosphate-buffered saline and homogenized in a hypotonic buffer (0.25 M sucrose, 20 mM HEPES pH 7.4, 2 mM EGTA, 1 mM phenylmethylsulfonyl fluoride, 10 μg/ml aprotinin, 10 μg/ml leupeptin, 10 μg/ml pepstatin). The homogenate (total cellular fraction) was clarified by centrifugation at 850 *g* for 15 min at 4°C; the resulting supernatant was then centrifuged at 100 000 *g* for 1 h at 4°C to isolate the membrane fraction as a pellet and the cytoplasmic fraction as the supernatant.

Brain nuclei were sedimented through a 2 M sucrose cushion. Brain areas from three animals were homogenized in 0.32 M sucrose, 10 mM Tris–HCl pH 7.4, 3 mM $MgCl_2$, 1 mM dithiothreitol, 0.1% Triton X-100, 10 μg/ml aprotinin, 10 μg/ml leupeptin and 10 μg/ml pepstatin by using a Potter homogenizer provided with a loosely fitting Teflon pestle. The homogenate was filtered through cheesecloth and centrifuged for 10 min at 1000 *g*. The pellet was resuspended in 3 ml of homogenization medium without Triton and supplemented with 1.9 M sucrose. This preparation was layered over a cushion of 2 M sucrose (10 ml) and centrifuged at 12 000 *g* in an HB4 rotor (Sorvall). The pellet was resuspended in 0.5 ml of 0.32 M sucrose. The purity of brain nuclei was assessed by light microscopy after crystal violet staining.

Tissue processing for electron microscopy

For electron microscopy, vibratome sections were used. Once immunostained, the sections were post-fixed in 2% OsO_4 for 1 h, dehydrated, embedded in araldite and flat-mounted in Formvar coated slides, using plastic cover-slips. After polymerization, selected areas were photographed, trimmed, re-embedded in araldite and re-sectioned at 1 μm. These semithin sections were re-photographed and resectioned in ultrathin sections. The ultrathin sections were observed in a Jeol electron microscope, without heavy metal staining to avoid artifactual precipitates.

Quantitation of β-catenin nuclear patches

β-catenin nuclear patches were quantitated at the electron microscope level in the dentate gyrus of wild-type and Tet/GSK-3β ($n = 2$) mice. For each animal, 10 electron micrographs (at ×3000) were taken per ultrathin section at the apex of the dentate gyrus. Quantitation was carried out on enlarged prints by two independent observers. In each print, the number of β-catenin nuclear patches and the number of nuclei with patches were counted and divided by the number of nuclei.

Supplementary data

For immunohistochemistry, LacZ staining, TUNEL and western blot procedures, see the Supplementary data, available at *The EMBO Journal* Online.

Acknowledgements

The authors would like to thank Drs Eric Kandel and Mark Mayford for the use of the CamKIIα-tTA mice; Drs Juan Lerma, Javier Díaz-Nido and Francisco Wandosell for helpful discussion and comments; Drs Filip Lim and Marina Sánchez for critical reading of this manuscript and for style correction; and Dr Ginés Morata for microscope and photography facilities. We are also grateful to Raquel Cuadros for technical assistance. This work was supported by an institutional grant from Fundación Ramón Areces, by a grant to J.A. from the Spanish CICYT, and by Neuropharma.

References

Alvarez,G., Munoz-Montano,J.R., Satrustegui,J., Avila,J., Bogonez,E. and Diaz-Nido,J. (1999) Lithium protects cultured neurons against β-amyloid-induced neurodegeneration. *FEBS Lett.*, **453**, 260–264.

Alzheimer,A. (1911) Über eigernartige krankhertsfülle des späteren alters. *Z. Gesamte Neurol. Psychiat.*, **4**, 356–385.
Anderton,B.H. (1999) Alzheimer's disease: clues from flies and worms. *Curr. Biol.*, **9**, R106–R109.
Baron,U., Freundlieb,S., Gossen,M. and Bujard,H. (1995) Co-regulation of two gene activities by tetracycline via a bidirectional promoter. *Nucleic Acids Res.*, **23**, 3605–3606.
Barth,A.I., Nathke,I.S. and Nelson,W.J. (1997) Cadherins, catenins and APC protein: interplay between cytoskeletal complexes and signaling pathways. *Curr. Opin. Cell Biol.*, **9**, 683–690.
Braak,E., Braak,H. and Mandelkow,E.M. (1994) A sequence of cytoskeleton changes related to the formation of neurofibrillary tangles and neuropil threads. *Acta Neuropathol. (Berl.)*, **87**, 554–567.
Brion,J.P., Tremp,G. and Octave,J.N. (1999) Transgenic expression of the shortest human tau affects its compartmentalization and its phosphorylation as in the pretangle stage of Alzheimer's disease. *Am. J. Pathol.*, **154**, 255–270.
Brownlees,J., Irving,N.G., Brion,J.P., Gibb,B.J., Wagner,U., Woodgett,J. and Miller,C.C. (1997) Tau phosphorylation in transgenic mice expressing glycogen synthase kinase-3β transgenes. *Neuroreport*, **8**, 3251–3255.
Busciglio,J., Lorenzo,A., Yeh,J. and Yankner,B.A. (1995) β-amyloid fibrils induce tau phosphorylation and loss of microtubule binding. *Neuron*, **14**, 879–888.
Duff,K. *et al*. (1996) Increased amyloid-β42(43) in brains of mice expressing mutant presenilin 1. *Nature*, **383**, 710–713.
Eger,A., Stockinger,A., Schaffhauser,B., Beug,H. and Foisner,R. (2000) Epithelial mesenchymal transition by c-Fos estrogen receptor activation involves nuclear translocation of β-catenin and upregulation of β-catenin/lymphoid enhancer binding factor-1 transcriptional activity. *J. Cell Biol.*, **148**, 173–188.
Ferreira,A., Lu,Q., Orecchio,L. and Kosik,K.S. (1997) Selective phosphorylation of adult tau isoforms in mature hippocampal neurons exposed to fibrillar Aβ. *Mol. Cell. Neurosci.*, **9**, 220–234.
Geula,C., Wu,C.K., Saroff,D., Lorenzo,A., Yuan,M. and Yankner,B.A. (1998) Aging renders the brain vulnerable to amyloid β-protein neurotoxicity. *Nature Med.*, **4**, 827–831.
Gingrich,J.R. and Roder,J. (1998) Inducible gene expression in the nervous system of transgenic mice. *Annu. Rev. Neurosci.*, **21**, 377–405.
Gomez-Isla,T., Hollister,R., West,H., Mui,S., Growdon,J.H., Petersen, R.C., Parisi,J.E. and Hyman,B.T. (1997) Neuronal loss correlates with but exceeds neurofibrillary tangles in Alzheimer's disease. *Ann. Neurol.*, **41**, 17–24.
Gossen,M. and Bujard,H. (1992) Tight control of gene expression in mammalian cells by tetracycline-responsive promoters. *Proc. Natl Acad. Sci. USA*, **89**, 5547–5551.
Gotz,J., Probst,A., Spillantini,M.G., Schafer,T., Jakes,R., Burki,K. and Goedert,M. (1995) Somatodendritic localization and hyperphosphorylation of tau protein in transgenic mice expressing the longest human brain tau isoform. *EMBO J.*, **14**, 1304–1313.
Gray,E.G., Paula-Barbosa,M. and Roher,A. (1987) Alzheimer's disease: paired helical filaments and cytomembranes. *Neuropathol. Appl. Neurobiol.*, **13**, 91–110.
Grundke-Iqbal,I., Iqbal,K., Tung,Y.C., Quinlan,M., Wisniewski,H.M. and Binder,L.I. (1986) Abnormal phosphorylation of the microtubule-associated protein tau (τ) in Alzheimer cytoskeletal pathology. *Proc. Natl Acad. Sci. USA*, **83**, 4913–4917.
Guenette,S.Y. and Tanzi,R.E. (1999) Progress toward valid transgenic mouse models for Alzheimer's disease. *Neurobiol. Aging*, **20**, 201–211.
Hall,A.C., Lucas,F.R. and Salinas,P.C. (2000) Axonal remodeling and synaptic differentiation in the cerebellum is regulated by WNT-7a signaling. *Cell*, **100**, 525–535.
Hardy,J. (1996) New insights into the genetics of Alzheimer's disease. *Ann. Med.*, **28**, 255–258.
Hetman,M., Cavanaugh,J.E., Kimelman,D. and Xia,Z. (2000) Role of glycogen synthase kinase-3β in neuronal apoptosis induced by trophic withdrawal. *J. Neurosci.*, **20**, 2567–2574.
Hoeflich,K.P., Luo,J., Rubie,E.A., Tsao,M.S., Jin,O. and Woodgett,J.R. (2000) Requirement for glycogen synthase kinase-3β in cell survival and NF-κB activation. *Nature*, **406**, 86–90.
Hong,M., Chen,D.C., Klein,P.S. and Lee,V.M. (1997) Lithium reduces tau phosphorylation by inhibition of glycogen synthase kinase-3. *J. Biol. Chem.*, **272**, 25326–25332.
Ishiguro,K., Shiratsuchi,A., Sato,S., Omori,A., Arioka,M., Kobayashi,S., Uchida,T. and Imahori,K. (1993) Glycogen synthase kinase 3β is identical to tau protein kinase I generating several epitopes of paired helical filaments. *FEBS Lett.*, **325**, 167–172.
Ishihara,T., Hong,M., Zhang,B., Nakagawa,Y., Lee,M.K., Trojanowski, J.Q. and Lee,V.M. (1999) Age-dependent emergence and progression of a tauopathy in transgenic mice overexpressing the shortest human tau isoform. *Neuron*, **24**, 751–762.
Klein,P.S. and Melton,D.A. (1996) A molecular mechanism for the effect of lithium on development. *Proc. Natl Acad. Sci. USA*, **93**, 8455–8459.
Lee,V.M., Balin,B.J., Otvos,L.,Jr and Trojanowski,J.Q. (1991) A68: a major subunit of paired helical filaments and derivatized forms of normal Tau. *Science*, **251**, 675–678.
Lovestone,S. *et al*. (1994) Alzheimer's disease-like phosphorylation of the microtubule-associated protein tau by glycogen synthase kinase-3 in transfected mammalian cells. *Curr. Biol.*, **4**, 1077–1086.
Lovestone,S., Hartley,C.L., Pearce,J. and Anderton,B.H. (1996) Phosphorylation of tau by glycogen synthase kinase-3β in intact mammalian cells: the effects on the organization and stability of microtubules. *Neuroscience*, **73**, 1145–1157.
Lucas,F.R. and Salinas,P.C. (1997) WNT-7a induces axonal remodeling and increases synapsin I levels in cerebellar neurons. *Dev. Biol.*, **192**, 31–44.
Manji,H.K., Moore,G.J. and Chen,G. (1999) Lithium at 50: have the neuroprotective effects of this unique cation been overlooked? *Biol. Psychiatry*, **46**, 929–940.
Masters,C.L., Simms,G., Weinman,N.A., Multhaup,G., McDonald,B.L. and Beyreuther,K. (1985) Amyloid plaque core protein in Alzheimer disease and Down syndrome. *Proc. Natl Acad. Sci. USA*, **82**, 4245–4249.
Mayford,M., Bach,M.E., Huang,Y.Y., Wang,L., Hawkins,R.D. and Kandel,E.R. (1996) Control of memory formation through regulated expression of a CaMKII transgene. *Science*, **274**, 1678–1683.
Metuzals,J., Robitaille,Y., Houghton,S., Gauthier,S., Kang,C.Y. and Leblanc,R. (1988) Neuronal transformations in Alzheimer's disease. *Cell Tissue Res.*, **252**, 239–248.
Miller,J.R. and Moon,R.T. (1996) Signal transduction through β-catenin and specification of cell fate during embryogenesis. *Genes Dev.*, **10**, 2527–2539.
Munoz-Montano,J.R., Moreno,F.J., Avila,J. and Diaz-Nido,J. (1997) Lithium inhibits Alzheimer's disease-like tau protein phosphorylation in neurons. *FEBS Lett.*, **411**, 183–188.
Murayama,M. *et al*. (1998) Direct association of presenilin-1 with β-catenin. *FEBS Lett.*, **433**, 73–77.
Nelson,P.T., Marton,L. and Saper,C.B. (1993) Alz-50 immunohistochemistry in the normal sheep striatum: a light and electron microscope study. *Brain Res.*, **600**, 285–297.
Pap,M. and Cooper,G.M. (1998) Role of glycogen synthase kinase-3 in the phosphatidylinositol 3-kinase/Akt cell survival pathway. *J. Biol. Chem.*, **273**, 19929–19932.
Papasozomenos,S.C. (1989) Tau protein immunoreactivity in dementia of the Alzheimer type: II. Electron microscopy and pathogenetic implications. Effects of fixation on the morphology of the Alzheimer's abnormal filaments. *Lab. Invest.*, **60**, 375–389.
Pei,J.J., Braak,E., Braak,H., Grundke-Iqbal,I., Iqbal,K., Winblad,B. and Cowburn,R.F. (1999) Distribution of active glycogen synthase kinase 3β(GSK-3β) in brains staged for Alzheimer disease neurofibrillary changes. *J. Neuropathol. Exp. Neurol.*, **58**, 1010–1019.
Price,D.L. and Sisodia,S.S. (1998) Mutant genes in familial Alzheimer's disease and transgenic models. *Annu. Rev. Neurosci.*, **21**, 479–505.
Selkoe,D.J. (1994) Normal and abnormal biology of the β-amyloid precursor protein. *Annu. Rev. Neurosci.*, **17**, 489–517.
Selkoe,D.J. (1998) The cell biology of β-amyloid precursor protein and presenilin in Alzheimer's disease. *Trends Cell Biol.*, **8**, 447–453.
Shiurba,R.A. *et al.* (1996) Immunocytochemistry of tau phosphoserine 413 and tau protein kinase I in Alzheimer pathology. *Brain Res.*, **737**, 119–132.
Spittaels,K. *et al*. (1999) Prominent axonopathy in the brain and spinal cord of transgenic mice overexpressing four-repeat human tau protein. *Am. J. Pathol.*, **155**, 2153–2165.
Stambolic,V., Ruel,L. and Woodgett,J.R. (1996) Lithium inhibits glycogen synthase kinase-3 activity and mimics wingless signalling in intact cells [published erratum appears in *Curr. Biol.*, 1997, **7**, 196]. *Curr. Biol.*, **6**, 1664–1668.
Takashima,A., Noguchi,K., Sato,K., Hoshino,T. and Imahori,K. (1993) Tau protein kinase I is essential for amyloid β-protein-induced neurotoxicity. *Proc. Natl Acad. Sci. USA*, **90**, 7789–7793.
Takashima,A., Noguchi,K., Michel,G., Mercken,M., Hoshi,M.,

Ishiguro,K. and Imahori,K. (1996) Exposure of rat hippocampal neurons to amyloid-β peptide (25–35) induces the inactivation of phosphatidyl inositol-3 kinase and the activation of tau protein kinase I/glycogen synthase kinase-3β. *Neurosci. Lett.*, **203**, 33–36.

Takashima,A. *et al*. (1998) Presenilin 1 associates with glycogen synthase kinase-3β and its substrate tau. *Proc. Natl Acad. Sci. USA*, **95**, 9637–9641.

Terry,R.D. (1998) The cytoskeleton in Alzheimer disease. *J. Neural Transm. Suppl.*, **53**, 141–145.

Weihl,C.C., Ghadge,G.D., Kennedy,S.G., Hay,N., Miller,R.J. and Roos,R.P. (1999) Mutant presenilin-1 induces apoptosis and downregulates Akt/PKB. *J. Neurosci.*, **19**, 5360–5369.

Woodgett,J.R. (1990) Molecular cloning and expression of glycogen synthase kinase-3/factor A. *EMBO J.*, **9**, 2431–2438.

Yamamoto,A., Lucas,J.J. and Hen,R. (2000) Reversal of neuropathology and motor dysfunction in a conditional model of Huntington's disease. *Cell*, **101**, 57–66.

Yankner,B.A. (1996) Mechanisms of neuronal degeneration in Alzheimer's disease. *Neuron*, **16**, 921–932.

Yu,G. *et al*. (1998) The presenilin 1 protein is a component of a high molecular weight intracellular complex that contains β-catenin. *J. Biol. Chem.*, **273**, 16470–16475.

Zhang,Z. *et al*. (1998) Destabilization of β-catenin by mutations in presenilin-1 potentiates neuronal apoptosis. *Nature*, **395**, 698–702.

Received August 23, 2000; revised October 18, 2000; accepted November 13, 2000